

# Enhancing Frequency Control through Rate of Change of Voltage Feedback

Federico Milano, *IEEE Fellow*, Bibi Alhanjari, Georgios Tzounas, *IEEE Member*

**Abstract**—This letter proposes a simple and inexpensive technique to improve the frequency control of distributed energy resources. The proposed control consists in modifying the conventional estimated bus frequency signal with an additional feedback signal that utilizes the rate of change of the voltage magnitude measured at the same bus. The case study showcases the benefits of the proposed control and compares its performance with standard frequency control schemes through time-domain simulations.

**Index Terms**—Frequency control, geometric observability, complex frequency, low-inertia systems.

## I. INTRODUCTION

The increasing proliferation of converter-based generation is known to reduce the available mechanical inertia in the electric power grid. As a result, frequency variations triggered from imbalances between power supply and demand become more prominent and faster, and threaten the system's stability and performance. In response to this challenge, system operators and researchers have been actively seeking for techniques that enhance the effectiveness of frequency control services provided by Distributed Energy Resources (DERs).

Literature in the field has explored several optimal control and coordination strategies for different converter-based energy technologies, including wind, solar PV, storage, and demand response systems [1], [2]. For example, recent works have proposed analytical methods for the design of synthetic inertia and droop coefficients of DERs to meet a desired dynamic performance, as well as optimal DER placement and power sharing strategies, e.g. see [3], [4].

In previous work, the authors of this paper have studied the analytical links between power, frequency and voltage variations in transmission and distribution networks to establish alternative control signals that can improve the stability and primary response of low-inertia systems [5], [6]. In this vein, this letter proposes to modify the bus frequency signal conventionally utilized in DER primary control loops to include as additional feedback signal the rate of change of the voltage magnitude measured at the same bus. The rationale of the proposed control scheme is based on a recent work by the first author that defines a novel quantity, namely, the *complex frequency*, where the rate of change of the voltage magnitude constitutes the real part and the conventional frequency is the imaginary part [7].

## II. RATIONALE AND PROPOSED CONTROL SCHEME

The definition of the complex frequency relies on a general property of complex quantities, as follows. Let us consider the Park vector of the bus voltage, say  $\bar{v}$ , as time-dependent complex value that utilizes the  $dq$ -axis components of the Park reference frame rotating at constant angular speed  $\omega_o$ , i.e:

$$\bar{v}(t) = v_d(t) + j v_q(t), \quad (1)$$

where  $j$  is the imaginary unit. This voltage is substantially a dynamic phasor and can be written in polar coordinates as:

$$\bar{v} = v e^{j\theta}, \quad (2)$$

F. Milano, B. Alhanjari and G. Tzounas are with the School of Electrical & Electronic Engineering, University College Dublin, D04V1W8, Dublin, Ireland. (e-mails: federico.milano@ucd.ie, bibi.ghjmalhanjari@ucdconnect.ie, georgios.tzounas@ucd.ie).

where we have dropped the dependency on time for economy in notation. Defining  $u = \ln(v)$ ,  $v \neq 0$ , (2) becomes:

$$\bar{v} = e^{u+j\theta}. \quad (3)$$

If  $\bar{v}$  is a function of time, then the derivative of (3) leads to:

$$\dot{\bar{v}} = (\dot{u} + j\dot{\theta}) e^{u+j\theta} = (\dot{u} + j\dot{\theta}) \bar{v}. \quad (4)$$

Equaling (2) and (1) and taking into account the rotation of the Park reference frame, one has:

$$\omega = \dot{\theta} = \frac{v_d \dot{v}_q - v_q \dot{v}_d}{v^2} + \omega_o, \quad (5)$$

$$\rho = \dot{u} = \frac{\dot{v}}{v} = \frac{v_d \dot{v}_d + v_q \dot{v}_q}{v^2}, \quad (6)$$

where  $\omega$  is the conventional instantaneous frequency of  $\bar{v}$  and  $\rho$  can be defined as an *instantaneous bandwidth* [8] or, using a geometric analogy, a *radial frequency* [9]. The time derivative of the Park vector in (1) can be written as:

$$\dot{\bar{v}} = (\rho + j\omega) \bar{v} = \bar{\eta} \bar{v}, \quad (7)$$

where  $\bar{\eta}$  is the *complex frequency* as defined in [7].

For the discussion of the control proposed in this letter, it is relevant to rewrite  $\omega$  and  $\rho$  in (5) and (6) assuming now that the Park transform is obtained using the frequency of the Center of Inertia (COI), say  $\omega_{COI}$ , rather than the synchronous reference frame  $\omega_o$ . This leads to:

$$\omega = \frac{v'_d \dot{v}'_q - v'_q \dot{v}'_d}{v^2} + \omega_{COI}, \quad (8)$$

$$\rho = \frac{v'_d \dot{v}'_d + v'_q \dot{v}'_q}{v^2}, \quad (9)$$

where  $v'_d + jv'_q$  is the Park vector obtained for the  $dq$ -axis reference frame rotating at  $\omega_{COI}$ .

While  $v'_d \neq v_d$  and  $v'_q \neq v_q$ , the values of  $\omega$  and  $\rho$  on the left-hand sides of (8) and (9) are in effect equal to the values in (5) and (6), respectively, as  $\omega$  and  $\rho$  are geometric invariants, that is, their values are independent from the coordinates utilized to measure the components of the voltage. The invariance of  $\rho$  is straightforward to show, as the identity  $v = |v_d + jv_q| = |v'_d + jv'_q|$  must hold independently of the reference speed chosen to obtain the Park transform. Demonstrating the invariance of  $\omega$  is more involved, and the interested reader can find a proof in [10].

The invariance of  $\omega$  and  $\rho$  leads to the following remarks:

- Equation (8) shows that the instantaneous frequency  $\omega$  can be decomposed into two terms. The first captures exclusively local bus dynamics and is null in steady state. The second, i.e.  $\omega_{COI}$ , is slow and follows the system-wide dynamic of the frequency.
- The radial frequency  $\rho$  depends only on local dynamics and, hence, is always null in steady state.

It is immediate to observe that, if the voltage at the bus where the frequency is measured is regulated through an automatic control, then the local variations of  $\rho$  can be relatively small w.r.t. the variations of  $\omega$ . An obvious limit case is that of an ideal voltage controller, for which  $\rho = 0$  as the voltage is always kept perfectly constant. This also justifies some models of the bus voltage signal proposed in the literature [11]. However, since ideal voltage controllers do not exist

in practice, we can always assume that the voltage magnitude and hence also  $\rho$  do exhibit a transient behavior following a disturbance.

In this letter we show the benefits for the frequency control of power systems of including  $\rho$  in the conventional frequency control input signal. Such control is meaningful when the dynamics of  $\omega$  and  $\rho$  evolve in similar time scales. This is particularly relevant for converter-interfaced devices, whose frequency controllers can be designed to be as fast or faster than their voltage regulation. We exploit this feature to design the proposed DER control. On the other hand, the proposed control is not suitable for conventional synchronous machines, as their voltage regulators are much faster than the dynamics that can be tracked by turbine governors.

A consequence of assuming similar time scales of frequency and voltage controllers is that the local terms of  $\omega$  and  $\rho$  in (8) and (9), while having different expressions, have similar harmonic content and thus, show a similar “trend”. This statement is further illustrated in the case study presented in Section III but we also justify it qualitatively below with an analytic example. Let us assume that:

$$\begin{aligned} v_d' &= V - k e^{-\alpha t} \cos(\beta t), \\ v_q' &= k e^{-\alpha t} \sin(\beta t), \end{aligned} \quad (10)$$

where  $V$ ,  $k$ ,  $\alpha$  and  $\beta$  are constant. The expressions in (10) resemble a typical frequency transient in power systems if  $k \ll V$  and  $\alpha, \beta \ll \omega_{COI}$ , where  $\alpha$  and  $\beta$  represent the damping and the angular frequency, respectively, of the dominant mode of the system. Leveraging these inequalities, one can get to the following approximated expressions from (8) and (9):

$$\begin{aligned} \omega - \omega_{COI} &\approx \frac{k e^{-\alpha t}}{V} [\beta \cos(\beta t) - \alpha \sin(\beta t)], \\ \rho &\approx \frac{k e^{-\alpha t}}{V} [\beta \sin(\beta t) + \alpha \cos(\beta t)]. \end{aligned} \quad (11)$$

The latter expressions show that  $\rho$  and  $\omega - \omega_{COI}$  have same order of magnitude and show same oscillatory behavior.

We use the observations and the empirical result above as follows. Conventional frequency controllers of non-synchronous resources utilize the estimation of the frequency of the voltage at their point of connection with the grid, e.g., using a Phased-Locked Loop (PLL), and compare it with a reference, typically  $\omega_o$ . The resulting frequency error signal is thus a mix of the local frequency oscillations and the system-wide frequency deviation due to the power imbalance in the grid. This means that the local and system-wide variations are weighted in the same way by the controller. This appears inevitable since, in order to estimate the local term of the instantaneous frequency in (8), one would need to be able to measure  $\omega_{COI}$  first, which is though not available to local controllers. However, extrapolating the result of the example above and based on the experience matured on a large number of simulations, we have observed that we can decouple, even if in an approximated way, these two effects and “weight” them differently in the frequency control.

The main advantage of the rate of change of voltage ( $\rho$ ) as compensating signal for the frequency control is that it is a purely local signal, as opposed to the frequency that is both local and system-wide as it intrinsically contains information on the frequency of the center of inertia ( $\omega_{COI}$ ). Controllers that utilize the rate of change of frequency (RoCoF) are effective as long as the variations of the RoCoF are not biased by the variations of  $\omega_{COI}$ . In conventional systems or systems where converters emulate the behavior and time scales of synchronous machines, e.g., [12], the variations of  $\omega_{COI}$  are slower than local frequency oscillations, and that is why controllers based on the RoCoF can be effective. However, in systems with very low inertia,  $\omega_{COI}$  can partially overlap with local fluctuations and thus lead to a less effective control based on the RoCoF. We note,

moreover, that controllers based on the RoCoF generally require an additional control channel in parallel with the conventional frequency droop control. On the other hand,  $\rho$  can be included in any existing DER frequency controller.

In summary, we propose to use  $\rho$  to build the following modified input signal to primary frequency controllers:

$$\tilde{\omega} = \omega - K \rho, \quad (12)$$

where  $K$  is the parameter to be adjusted and that allows tuning the impact of local frequency oscillations on the power output of the converter-interfaced device. It is relevant to observe that the estimation of  $\rho$  is simple and readily available as, from (6), one simply needs to measure  $v$  and estimate  $\dot{v}$ .

### III. CASE STUDY

In this section, we illustrate the effect of the proposed control with the WSCC 9-bus system and the New England 39-bus system. All simulation results are obtained with the software tool Dome [13]. In the simulations, estimations of  $\omega$  and  $\rho$  are obtained using a synchronous-reference frame PLL and voltage measurements at the point of connection of the converter-interfaced generator (CIG).

#### A. WSCC 9-bus System

The original WSCC 9-bus system is modified to emulate a low-inertia system by reducing the inertia constants of the synchronous machines (SMs), namely, 4 s for SM 1 and 2 and 3 s for SM 3. Then, a CIG is connected through a transformer to bus 7. The block diagram of the CIG control is shown in Fig. 1. The inner loop regulates the  $dq$ -axis currents and includes limiters. The outer loop consists of a voltage controller and a frequency controller with droop and washout channels. In the scheme,  $p^{\text{ref}}$  and  $q^{\text{ref}}$  are the operating set points for a given period of the DER as defined by the market and/or transmission system operators; whereas  $v_{\text{POD}}^{\text{ref}}$  is an auxiliary signal coming from power oscillator damper (POD) connected to the DER, which is equivalent of the power system stabilizers of conventional synchronous generators. The considered DER utilizes a grid-following converter. It is important to note that employing grid-forming converters would not change the effectiveness of the proposed compensating signal based on  $\rho$  as long as the voltage and frequency controllers have similar time scales. At the initial operating point the CIG generates 100 MW, which are accommodated in the system by reducing by the same amount the power produced by SM 2.

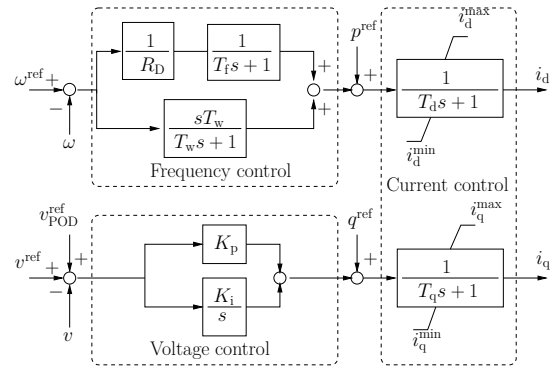


Fig. 1. Control diagram of the primary controllers of DERs. The conventional frequency controller utilizes the signal  $\omega$ , whereas the proposed control utilizes as input signal  $\tilde{\omega}$  as defined in (12).

To study the effectiveness of the proposed control in improving the frequency response of the system, we first compare the observability that the signals  $\omega$  and  $\tilde{\omega}$  provide to the dynamic modes of the system

TABLE I  
GEOMETRIC OBSERVABILITY  $go$  OF FREQUENCY CONTROL MODE.

Signal	$\rho$	$\omega$	$\tilde{\omega} = \omega - \rho$
Observability	0.34	0.87	1.00

directly linked to primary frequency regulation. Recall that a dynamic mode represents a primary frequency control mode if it meets the following properties [14]: (i) it is global, i.e. all buses are coherent to the mode. (ii) the associated mode shapes for all generator speeds are in phase; and (iii) its natural frequency lies in the range 0.02-0.1 Hz.

We carry out a small-signal analysis of the system assuming that the CIG frequency control loop is switched off. The results indicate that the system is stable at the examined equilibrium and that the primary frequency control mode is represented by the complex pair of eigenvalues  $-0.55 \pm j1.12$  with natural frequency 0.09 Hz. The corresponding normalized mode shapes of the rotor speeds of the three SMs are depicted in the left panel of Fig. 2.

The geometric observability  $go$  [15] of the frequency control mode by  $\rho$ ,  $\omega$ , and  $\tilde{\omega}$  for  $K = 1$ , are summarized in Table I. The right panel in Fig. 2 tracks the ratio  $go(\tilde{\omega})/go(\omega)$  between the observability of  $\tilde{\omega}$  and  $\omega$ , as a function of  $K$ . This analysis confirms that  $\rho$  is effective to improve the dynamic behavior of the system. Note, however, that the specific value of the gain depends on the estimation of  $\rho$ , which in the simulations below is obtained through a PLL that estimates  $\dot{\psi}$ , and the parameters of the frequency controller of the CIG.

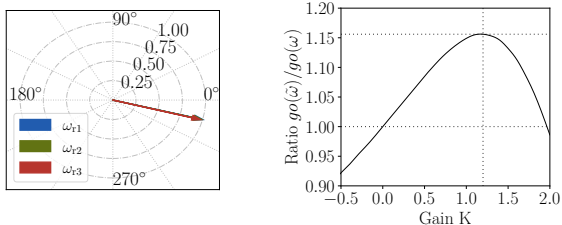


Fig. 2. WSCC test system: Left: Frequency control mode shapes of SM speeds. Right: geometric observability ratio for the conventional and proposed frequency control modes as a function of  $K$ .

Figures 3 and 4 show the transient behavior of the system following the loss of 50% of the load consumption at bus 5, for three scenarios: (i) system without CIG; (ii) system with CIG and frequency control using the conventional signal  $\omega$ ; and (iii) system with CIG and frequency control using the proposed signal  $\tilde{\omega}$  defined in (12). The results shown in Figs. 3 and 4 were obtained for  $K = 1.2$ .

The proposed control achieves lower deviations of the COI frequency and of the power generated by the CIG, without deteriorating the voltage control performance or modifying the reactive power output. The compensating signal has the sought effect of reducing the local oscillation of the active power of the CIG, which results in an overall improvement of the system frequency dynamic response.

### B. New England 39-bus System

This section illustrates the dynamic performance of the proposed control for a larger system with multiple CIGs. The original data is modified to accommodate 70% of CIG-based generation and the inertias of conventional SMs are reduced to emulate a low-inertia system. The setup of the grid is same as in [6]. The contingency considered is a fault at bus 12 cleared after 0.2 s. Figure 5 shows that, also in this case, the compensating signal effectively reduces local oscillations and improves the system frequency dynamic response.

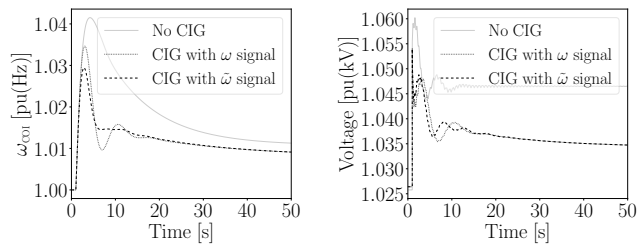


Fig. 3. Transient behavior of the frequency of the COI and of the voltage at bus 7 for various control setups of the WSCC test system.

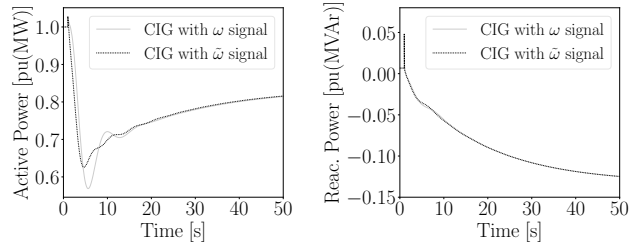


Fig. 4. Transient behavior of the power injected by the CIG for various control setups of the WSCC test system.

It is relevant to note that, in this scenario, the signal  $\tilde{\omega}$  is obtained using  $K = -0.03$ . Comparing this value with that utilized for the WSCC 9-bus system ( $K = 1.2$ ), we note that the gain  $K$  is highly system-dependent and can be positive or negative. On the other hand,  $K$  does not need to be adjusted when the operating point changes and, according to our study, does not appear to interfere or couple with other system dynamics.

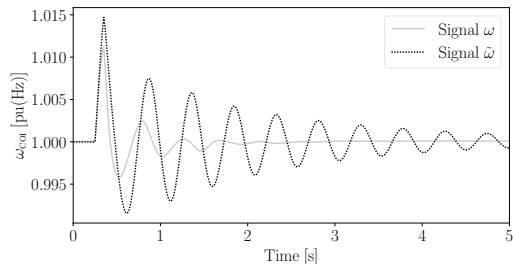


Fig. 5. New England 39-bus system: Transient behavior of the frequency for various setups of the frequency control of the CIGs.

## IV. CONCLUSIONS

This letter builds on top of a recently proposed definition of *complex frequency* that accounts for angle and magnitude voltage rate of changes in a unified geometric-based framework. The invariant properties of the components of the complex frequency are exploited in this work to separate local and system-wide dynamics of the frequency. This separation allows defining a frequency control that can compensate local oscillations and, as a consequence, improve the overall transient response of the grid. The effectiveness of this approach is confirmed by the eigensensitivity analysis and the evaluation of the geometric observability of the proposed compensated control signal, and by time-domain simulations. The proposed control is suited for CIGs, the active power controllers of which are generally faster than those of conventional power plants and are thus more prone to be affected by local oscillations of the frequency. Finally, the proposed control is also simple and inexpensive to implement as it requires only local measurements of the voltage at the point of connection of the devices that regulate the frequency.

## REFERENCES

- [1] H. Bevrani, H. Golpira, A. R. Messina, N. Hatziaargyriou, F. Milano, and T. Ise, "Power system frequency control: An updated review of current solutions and new challenges," *Electric Power Systems Research*, vol. 194, p. 107114, 2021.
- [2] Z. A. Obaid, L. M. Cipcigan, L. Abraham, and M. T. Muhssin, "Frequency control of future power systems: reviewing and evaluating challenges and new control methods," *Journal of Modern Power Systems and Clean Energy*, vol. 7, no. 1, pp. 9–25, 2019.
- [3] S. S. Guggilam *et al.*, "Optimizing DER participation in inertial and primary-frequency response," *IEEE Trans. on Power Systems*, vol. 33, no. 5, pp. 5194–5205, 2018.
- [4] B. K. Poolla, D. Groß, and F. Dörfler, "Placement and implementation of grid-forming and grid-following virtual inertia and fast frequency response," *IEEE Transactions on Power Systems*, vol. 34, no. 4, pp. 3035–3046, 2019.
- [5] G. Tzounas and F. Milano, "Improving the frequency response of DERs through voltage feedback," in *2021 IEEE Power Energy Society General Meeting (PESGM)*, 2021, pp. 1–5.
- [6] F. Sanniti, G. Tzounas, R. Benato, and F. Milano, "Curvature-based control for low-inertia systems," *IEEE Transactions on Power Systems*, vol. 37, no. 5, pp. 4149–4152, 2022.
- [7] F. Milano, "Complex frequency," *IEEE Transactions on Power Systems*, vol. 37, no. 2, pp. 1230–1240, 2022.
- [8] L. Cohen, *Time-Frequency Analysis: Theory and Applications*. Upper Saddle River, NJ: Prentice-Hall Signal Processing, 1995.
- [9] F. Milano, G. Tzounas, I. Dassios, and T. Kërçi, "Applications of the Frenet frame to electric circuits," *IEEE Trans. on Circuits and Systems I: Regular Papers*, pp. 1–13, 2021.
- [10] F. Milano, "A geometrical interpretation of frequency," *IEEE Trans. on Power Systems*, vol. 37, no. 1, pp. 816–819, 2022.
- [11] A. Karpilow, A. Derviškadić, G. Frigo, and M. Paolone, "Characterization of non-stationary signals in electric grids: A functional dictionary approach," *IEEE Transactions on Power Systems*, vol. 37, no. 2, pp. 1126–1138, 2022.
- [12] U. Markovic, Z. Chu, P. Aristidou, and G. Hug, "LQR-based adaptive virtual synchronous machine for power systems with high inverter penetration," *IEEE Transactions on Sustainable Energy*, vol. 10, no. 3, pp. 1501–1512, 2019.
- [13] F. Milano, "A Python-based software tool for power system analysis," in *IEEE PES General Meeting*, 2013, pp. 1–5.
- [14] A. Moeini and I. Kamwa, "Analytical concepts for reactive power based primary frequency control in power systems," *IEEE Transactions on Power Systems*, vol. 31, no. 6, pp. 4217–4230, 2016.
- [15] Milano, F., Dassios, I., Liu, M., and Tzounas, G., *Eigenvalue Problems in Power Systems (1st ed.)*. CRC Press, 2021.